

Equation of state, radial flow, and freeze-out in high energy heavy ion collisions

C. M. Hung and E. Shuryak

Physics Department, State University of New York at Stony Brook, New York 11794-3800

(Received 29 October 1997)

We have shown that recent experimental data on radial flow, both from AGS and SPS energies, are in agreement with the equation of state (EOS) including the QCD phase transition. A new hydrokinetic model (HKM) is developed, which incorporates a hydrodynamical treatment of the expansion and proper kinetics of the freeze-out. We show that the freeze-out surfaces for different secondaries and different collisions are very different, and they are not at all isotherms $T=\text{const}$ (as was assumed in most previous hydrodynamics works). Comparison of HKM results with the cascade-based event generator RQMD is also made in some detail: we found that both the EOS and flow are in rather good agreement, while the space-time picture is still somewhat different. [S0556-2813(98)05504-6]

PACS number(s): 25.75.Ld, 12.38.Mh, 21.65.+f

I. INTRODUCTION

One of the main physics goals of high energy nuclear collisions includes a test of whether for *heavy* enough ions at the AGS/SPS energy range (10–200 GeV/nucleon) production of (locally) equilibrated hot and dense hadronic matter really takes place. We do know that at the early stages of those collisions (a few fm/c after the first impact) a very large energy density of the order of several GeV/fm³ is actually reached. How rapidly it is equilibrated and whether a new phase of matter—quark-gluon plasma (QGP)—is indeed produced remain unclear. One possible strategy to answer those questions is relying on special rare processes happening at earlier stages, the electromagnetic probes [1], or J/ψ suppression [2]. In both directions we have recent exciting experimental findings [3,4].

This work is, however, devoted to hadronic observables related to production of the usual secondaries π, N, K , etc. It is widely believed that their spectra are not actually sensitive to questions mentioned above: and indeed, as the produced multiparticle system expands and cools, the rescattering erases most traces of the dense stage. Nevertheless, those which are *accumulated* during the expansion remain, and thus provide valuable information about the state of matter through its evolution.

The central phenomenon of such a kind discussed in this paper is a *collective flow*. Its multiple studies at Bevalac and SIS energies ($E/A \sim 1$ GeV) have shown a number of interesting effects. However, it was concluded that nuclear matter does not really reach equilibration under such conditions.

In contrast to that, in high energy pp (or even e^+e^-) collisions, the thermal description for particle spectra and composition works surprisingly well [6,7]. At the same time (except maybe at very high energies), there is *no* observed

collective radial flow in these cases (see [8] and the next section): this alone shows that the system is not truly macroscopic.¹

In contrast to that, data for heavy ion collisions show very strong flow, therefore suggesting that the excited system created does indeed behave as a truly macroscopic system. To test whether it is indeed so is the main *physics* objective of this paper. More specifically, we study whether available experimental data on heavy ion collisions in the AGS and SPS energy domain are consistent with (so far semiquantitative) information about the equation of state (EOS) of hot and dense hadronic matter as obtained from current lattice QCD.

The central phenomenon studied in this work is the so-called *radial* (or axially symmetric) flow, observed in central collisions. Current data are now rich enough to allow systematic study of its collision energy and rapidity dependence, as well as dependence on the nuclear size (A dependence) and the particular secondary particle involved. All those dependencies are discussed below, and to a large extent reproduced by our model.

Another, more *practical* objective of this paper is to create a *next generation* model for heavy ion collisions, to be called hydrokinetic model (HKM). It incorporates three basic elements of the macroscopic approach: (i) thermodynamics of hadronic matter, (ii) hydrodynamics of its expansion, and (iii) realistic hadronic kinetics at the freeze-out. Most elements of the model have in fact been worked out in literature, and some are new, but we think they are taken together for the first time.

The hydrodynamics-based works available in the literature² aimed more at a proper parametrization of the initial conditions [9], which would then lead to y, p_t spectra comparable with the data. Among recent papers let us mention [11] which studied the first few fm/c and attempted to

¹An explanation suggested in [8] is that in pp/e^+e^- collisions matter excitation is not strong enough to overcome the “bag pressure,” and small systems created have stabilized transverse size at some equilibrium value, and thus zero pressure. Modern models explaining these data use strings: those are precisely such objects. Large systems created in nuclear collisions must have positive pressure, and thus expand.

²After a very long break, there was a workshop in Trento ECT, 1997 devoted entirely to this subject. Its proceedings (which will appear as a series of papers in the journal Heavy Ion Physics) should give a rather complete description of recent activities.

derive the initial conditions from a three-liquid model and [13] which has studied some specific EOS-related observables. Probably the closest in spirit to our work is a recent paper [14], in which the same freeze-out condition is used. Unfortunately, its physical consequences are not studied in any detail, and their method (referred to as “global” hydrodynamics) includes unnecessary averaging, which significantly obscures them. To the extent we could trace them, our findings actually qualitatively agree with the results of [14]. In particular, we also found that the resonance gas EOS leads to too strong a flow at SPS, while the softer EOS including the phase transition gives it about right.

Let us now comment on the relations between our approach and the widely used cascade “event generators” (Fritjof, Venus, RQMD, ARC, etc.). Hydrodynamics and cascades were often treated as alternatives, and many scientists trust cascades much more, as those are “based on known physics.” In reality, both rather should be used as complementary tools.

The very fact that all event generators approximately work, in spite of huge differences between them (their tables of cross sections, lists of resonances included, etc., are different, some have strings or even color “ropes”), indicates that bulk results are insensitive to those differences. For example, particle composition appears to be rather well equilibrated, explaining the insensitivity to details of the model in some observables. The simplest way to test which of those parameters are relevant is to vary the input parameters: unfortunately, very little work has been so far done along this line. Considering flow, one should obviously have a look at components of the stress tensor, the pressure p , and energy density ϵ . Hadronic cascades (see [28] for RQMD) have a very simple EOS, $p/\epsilon \approx \text{const}$, typical of thermal resonance gas (see below).

Obviously cascades have a lot to say about *later* stages of the collisions, at the so-called freeze-out stage where interactions stop, resonances decay, etc. They also provide more detailed information (e.g., the degree of local chemical and thermal equilibration) which in principle³ helps us understand the validity limits of the macroscopic variables and approaches. We will discuss many of these issues below.

At the same time, a description based on the hadronic cascade of the *earlier* stages of the collisions obviously has little theoretical justification, and fails in practice for sufficiently high energies (SPS). “Event generators” therefore rely on specific models (color strings and their breaking, etc.), introducing plenty of unknown parameters or even concepts (e.g., “color ropes”). What is even worse, these models have so far no connection to developments in nonperturbative QCD, say, to lattice studies of QCD thermodynamics. They disregard such issues as chiral restoration and deconfinement, leading to the disappearance of the very objects

³In practice, to our knowledge it was not even demonstrated that any of these cascade codes satisfy the detailed balance (say there are resonance decays and other two to many hadronic processes without their inverse), and that, even if given time, they do lead to correct thermal equilibrium.

they work with, hadrons and strings.⁴ The hydrodynamics description, on the other hand, is much simpler and operates directly with the EOS, so in this framework, one can easily incorporate different scenarios (e.g., with or without the QCD phase transition).

Our last comment is practical: with experiments proceeding from light ions to heavy ones, and from the AGS and SPS to the RHIC and LHC energies we have to deal with many thousands of secondaries. Direct simulation of all their rescattering is neither practical nor necessary: as soon as the system is much larger than the interaction range, the system can be cut into parts (or “cells”) which evolve independently from each other. Furthermore, one may separate internal evolution (thermodynamics and kinetics) from the cell’s motion (hydrodynamics), enormously simplifying the problem. As multiplicities grow cascades become more and more expensive, while the macroscopic approach becomes only more accurate: at some point going from one language to another becomes inevitable.

This paper is structured as follows. In Sec. II we start with some phenomenological introduction into the properties of the radial flow, setting the problem to be discussed below. In Sec. III we consider the thermodynamics of hadronic matter, using a rather standard model of resonance gas plus QGP with bag-model EOS. The important step is the determination of the particular paths the volume elements of matter make in the phase diagram (e.g., temperature T , baryonic chemical potential μ_b) during expansion. Then we determine the effective EOS on these paths, to be used in Sec. IV in hydrodynamics calculations. In this paper we will not discuss nonequilibrium phenomena neither at the formation stage nor during the passage of the phase transition. It is more important, however, to address kinetic phenomena at the end of hydroexpansion, the so-called *freeze-out* stage: this we do in considerable detail in Sec. V. Here we separately discuss chemical and thermal freeze-out and discuss how the final spectra of secondaries are generated. Then we go to a comparison of observables, and especially the radial flow, with experiment and cascades (RQMD); see Sec. VI. A summary of the paper is contained in Sec. VII.

II. FLOW: THE PHENOMENOLOGICAL INTRODUCTION

First of all, in order to put things into proper perspective and introduce the terminology, we recall that the collective flow can be observed as follows. (i) Axially symmetric *radial* and (ii) *longitudinal* flow exist even for central collisions. For nonzero impact parameter experiments have also shown clear signals for at least two nonzero harmonics in the angle ϕ , known as (iii) *dipole* and (iv) *elliptic* flow.

In this paper we study only the first of them, the radial flow, and so let us now comment on others. The longitudinal flow was studied a lot in other hydrodynamics-based works [9]: we decided not to discuss it here in detail. It is a parametrization rather than a real prediction: the issue is obscured by an uncertainty in initial conditions.

⁴Therefore their phenomenological success is even used as an argument against the reality of the QCD phase transition itself: needless to say, we are strongly opposed to this point of view.

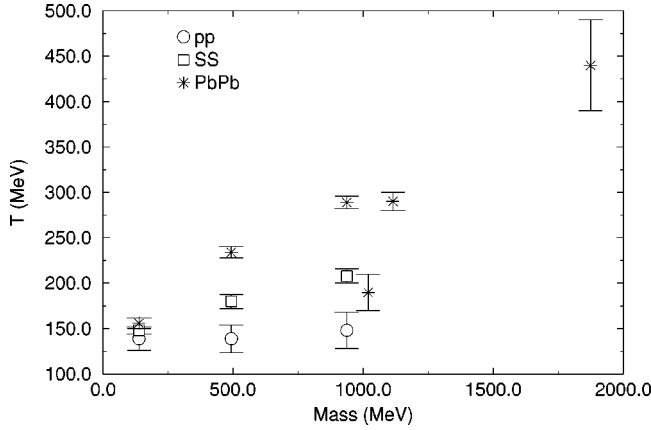


FIG. 1. Experimentally measured slopes of m_t distributions as a function of particle mass (MeV), for π, K, N (NA44) and ϕ, Λ, d (NA49), in acceptance of these experiments. Three types of points correspond to pp , SS , and $PbPb$ collisions.

Asymmetric flow (iii) and (iv) is potentially very interesting, especially the elliptic one [15,16]. The difference between the elliptic and radial flow should mostly appear due to earlier stages: it is obviously an exciting subject for further work. (At the moment we however feel that it is too early; one should be able to get more details from experiment first. For a recent summary see [17]).

The existence of radial flow in nuclear collisions was widely debated in the literature for a decade. Phenomenological fits of the p_t spectra of various secondaries by some (*ad hoc*) velocity profile (or even a single velocity value v_t) and the *same* decoupling temperature T_f are possible: see [10]. Unfortunately, the data allow for multiple fits, with a wide margin for the trade-off between v_t and T_f . In particular, for heavy ions one can obtain equally good fits with ($T_f=140$ MeV, $v_t=0.4$) and ($T_f=120$ MeV, $v_t=0.6$). However, as we will show below, the model used was oversimplified. Even the main assumption that one should expect the same v_t and T_f for all secondaries is in obvious contradiction of the elementary kinetics of the freeze-out.

More important is that rich experimental systematics is now emerging. In Fig. 1 we show a collection of slopes from NA44 [5] and NA49⁵ experiments at SPS, for $\pi, K, N, \phi, \Lambda, d$. The definition is⁶

$$E \frac{dN}{d^3p} = C(y) \exp\left(-\frac{m_t}{\tilde{T}(y)}\right), \quad m_t^2 = p_t^2 + m^2. \quad (1)$$

One major observation is a very strong *mass dependence*: the slopes show consistent growth with the particle mass. It is clear how collective flow may explain it: for heavier secondaries, the thermal motion is smaller and the collective veloc-

ity v_t starts to show up. (Or, alternatively, collective motion generates a larger momentum mv_t for larger m .)

Note, however, that there are no lines on this plot. As will be clear from what follows, we do not believe in any simple m dependence of the slope: participation in flow takes place until decoupling of the particular particle, which depends on its scattering rates. Excellent examples of that are provided by strange hadrons. Accurate slopes for $\phi, \Lambda, \Xi, \Omega$ are coming from current experiments, but are not yet available. As all of them have smaller cross sections for collisions with low energy pions (e.g., a completely strange Ω cannot make resonances with pions) earlier decoupling is expected. As a result, smaller flow should be observed. (If, on the contrary, the increased slopes are due to *initial* state scattering, as advocated, e.g., in [22], one should instead get a larger slope for strange particles, since they are not stopped by a ‘‘friction force’’ in matter later.)

Another excellent test for the existence of the flow is provided by deuterons. The shape of their spectrum, slope \tilde{T}_d , and even yield are all very sensitive to the magnitude of the flow. For example, if flow is absent and both protons and neutrons are produced independently, with a distribution $\sim \exp(-p_t^2/2m_N T_N)$, their coalescence into d would generate a distribution with the *same* $\tilde{T}_d = \tilde{T}_N$. The observed value is much larger. The flow implies a specific correlation between position and momentum, which helps to produce a larger p_t . If this correlation is artificially removed (see [26], where in the RQMD output the nucleon’s positions or momenta were interchanged) the deuteron spectra change shape and their yield drops.

The next point is a strong A dependence, also quite evident from Fig. 1. While the pp data show perfect thermal-looking spectra without a slightest trace of radial flow [8], for SS collisions the slopes start growing with the mass of the secondary particle, and for $PbPb$ the effect is about twice as large. So the larger the nuclei, the stronger is the flow.

This point is very important, because such a trend qualitatively contradicts what most of the hydrodynamics models in the literature would obtain. The initial longitudinal size is usually taken to be either (i) the same for all or (ii) it scales as $A^{1/3}$. With such assumptions and A -independent freeze-out temperature one gets either (i) a system which looks more and more one dimensional, with the radial flow *decreasing* with A , or (ii) a system with a geometric scaling,⁷ with A -independent flow. The observed flow is *increasing* with A , and naturally follows from improved freeze-out conditions to be discussed below.

One more aspect of the systematics of the radial flow is their *rapidity* dependence. The nucleon slopes (taken from [29]) from E877 and E866 experiments at AGS are compiled in Fig. 2. One can clearly see from it that strong flow (and presumably its A dependence) comes preferentially from the central region, $y \sim 0$ (in the center of mass frame).

⁵A disclaimer: NA49 data we use are very preliminary [21], and are presented here for qualitative comparison only. Note that NA49 has the rapidity coverage wider than NA44, and therefore their slopes are (and should be) somewhat smaller.

⁶The tilde should remind the reader that slopes are not temperatures, as they also include the effect of the flow and resonance decays.

⁷Note that hydrodynamics equations are invariant if one changes all coordinates t, z, r by some common factor. So if all initial conditions are simply rescaled by a common factor like $A^{1/3}$, the expansion time changes accordingly and the velocity at the same iso-therms does not change.

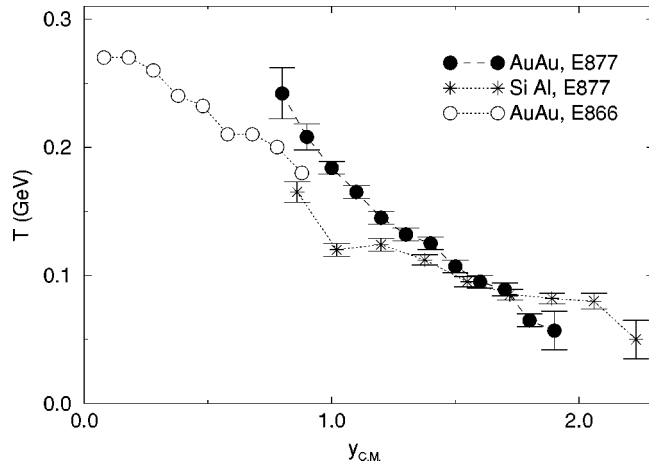


FIG. 2. Experimentally measured proton slopes of m_t distributions at AGS as a function of rapidity y (counted from CM).

Compared to these strong trends, the observed dependence of the flow on the *collision energy* appears to be weak. Unlike for Bevalac and SIS energies, in which v_t steadily grows, for the AGS (10–15 GeV/nucleon) and SPS (160–200 GeV/nucleon) domain the radial flow velocity is (inside uncertainties) about the same. It must be a mere coincidence, since the meson/baryon ratio, the EOS, and even the general picture of the space-time development of the collisions are radically different. Furthermore, as we have shown previously [45], hydrodynamics predicts a rather nonmonotonous dependence of the lifetime of the excited matter as a function of the collision energy, with a sharp maximum between AGS and SPS energies. This long time is related to a rather specific “burning pancake” regime: and although no detailed calculation of radial flow was made, it is hard to see how it can avoid having some kind of discontinuity as well. The simplicity⁸ of the model used in [45] somewhat limited its predictive power; we believe the main conclusion about the peak of the lifetime should persist. One can look for this effect experimentally by scanning to lower energies at SPS or by scanning various impact parameters. (Although we have not studied noncentral collisions in this work, it is probably worth mentioning that such a scan for J/ψ suppression has shown discontinuous behavior at about the same energy density.)

Another interesting manifestation of the “softness” of the EOS is stabilization of the radial flow at much higher RHIC energies. In this case hydrodynamics predicts a “burning log” picture [33], leading to a mixed phase surviving for 25–30 fm/c. As we will show shortly, this regime actually appears at SPS energies already.

III. THERMODYNAMICS OF HADRONIC MATTER

A. Quark-gluon plasma

Unlike real experiments, numerical ones performed on the lattice are easier to do at higher T . As a result, current lattice data have significantly clarified the QCD thermodynamics of

⁸The EOS had no baryon number and full stopping was assumed, which may not be the case even for the heaviest nuclei.

the quark-gluon plasma phase. Above the phase transition region (see below) the thermodynamics was found to be close to that of an ideal quark-gluon gas. Deviations are a typically 10–15 % downward shift in pressure and energy density p, ϵ [23], which are roughly reproduced by the lowest order [$O(g^2)$] perturbative corrections.⁹ Since for hydrodynamics only the p/ϵ ratio matters, this common factor can safely be ignored. The nonperturbative corrections are more important: they are well seen in lattice data for $T=(1-2)T_c$. Following tradition, we parametrize it simply by addition of the bag-type term B to the EOS of an ideal quark-gluon plasma:

$$\epsilon = \frac{\pi^2 T^4}{15} \left(16 + \frac{7}{8} 6N_f \right) + \frac{3N_f}{2} \left(T^2 \mu_b^2 + \frac{\mu^4}{2\pi^2} \right) + B,$$

$$p = \frac{\pi^2 T^4}{45} \left(16 + \frac{7}{8} 6N_f \right) + \frac{N_f}{2} \left(T^2 \mu_b^2 + \frac{\mu^4}{2\pi^2} \right) - B. \quad (2)$$

The value of B is tuned to get $T_c = 160$ MeV for zero baryon density (see below), resulting in the value¹⁰ $B = 320$ MeV/fm³.

Lattice data are also displaying a very spectacular phase transition in the vicinity of T_c , in which ϵ grows by a large factor. Although the exact dependence of the order of the transition on the theory parameters (such as quark masses, number of colors and flavors) is still far from being completely clarified (see [23,24] for recent review), it is already quite clear that in a practical sense the transition is close to the first order one with large latent heat. Whether there is a real jump or just a rapid rise inside a few MeV range of T can hardly be practically relevant: a high accuracy of T cannot be reached for the finite-size systems we work with.

The actually relevant variable is not T but ϵ : and below we would refer to matter in a wide range of energy densities $\epsilon \sim 0.3-1.5$ GeV/fm³ as a “mixed phase” domain. Its precise structure remains unknown: but fortunately it should not matter for hydrodynamics, provided the inhomogeneous domains (known also as “bubbles” of QGP) do not become too large. Fortunately, the hint we have from lattice data is a predicted tiny value (about 1% of T_c^3) for the surface tension. If it is true, the boundaries between the two phases cost little energy, and so this phase should be very well mixed indeed.

B. Hadronic matter as a resonance gas

Ironically enough, the properties of the hadronic matter at $T < T_c$ are theoretically understood much less than of QGP. In many applications scientists usually simply used the ideal pion gas as the simplest model: it leads then to a huge latent heat in the transition. However, this approach is clearly inadequate, and many more hadronic degrees of freedom are actually excited.

⁹All higher orders which can be perturbatively calculable have been now calculated, but those showing a divergent (or at least nonconvergent) series, with large and alternating sign terms.

¹⁰Note that it is about 6 times the original constant of the MIT bag model, and also only about a 1/2–1/3 of what one would get if all gluon condensates were eliminated.

We use instead the *resonance gas* approach, suggested very early by Landau and Belenky [18]. They have shown, using the lowest order virial expansion, that resonances¹¹ seen in scattering phases in fact contribute to thermodynamical parameters exactly as stable particles. It was later used by Hagedorn in his statistical bootstrap studies of the 1960's: his main point was that the *exponential* mass spectrum leads to the upper possible temperature of the hadronic gas. However, it was noticed by one of us long ago [25] that the observed resonance mass spectrum can better be fitted by the power of the mass than the exponent. It leads to a rather simple EOS, for zero baryon number $p, \epsilon \sim T^6$ [25] or $p \approx 0.2\epsilon$. Later much more detailed calculations with actual scattering phases confirmed it.

In this work we also include a nonzero baryon density, and so our thermodynamics has two variables T and μ_b .¹² Except at low energies (when we are close to nuclear matter), we know very little about the role of nonzero baryon density in the EOS. As is well known, lattice calculations are so far impossible in this case, due to the complex weight function for the nonzero chemical potential.

A simple generalization of the resonance gas to the nonzero chemical potential is of course natural, but it is known to have a problem at low T and high density. The naive Fermi gas for nucleons clearly overestimates the pressure of nuclear matter. The QGP with a reasonable bag constant cannot compete with it, and therefore a phase transition line has a pathological behavior at $\mu > 0.8$ GeV [see dotted line in Fig. 3(a)]. Following many others (e.g., [27]) we have solved this problem by the excluded volume correction, which effectively reduces the baryonic pressure at high μ . Specifically we adopted the excluded volume model in [40], which is thermodynamically consistent, and is characterized by the canonical partition function

$$Z^{\text{excl}}(T, \{N_i\}, V) = \sum_i Z(T, N_i, V - V_0 N_i) \theta(V - V_0 N_i),$$

from which

$$\begin{aligned} P^{\text{excl}}(T, \{\mu_i\}) &= \sum_i P_i^{\text{ideal}}(T, \mu_i - V_0 P^{\text{excl}}(T, \{\mu_i\})) \\ &= \sum_i P_i^{\text{ideal}}(T, \tilde{\mu}_i). \end{aligned}$$

V_0 is the excluded volume, which we assume to be the same for all fermions, while $V_0 = 0$ for bosons,

$$n_i^{\text{excl}}(T, \{\mu_i\}) = \left(\frac{\partial P^{\text{excl}}}{\partial \mu_i} \right)_{T, \{\mu_j\} \setminus \mu_i} = \frac{n_i^{\text{ideal}}(T, \tilde{\mu}_i)}{1 + V_0 \sum_j n_j^{\text{ideal}}(T, \tilde{\mu}_j)},$$

¹¹Those should be narrow enough: $\Gamma \ll T$.

¹²The chemical potential for strangeness μ_s is a *dependent* variable, with its value always fixed from the total strangeness $S=0$ condition.

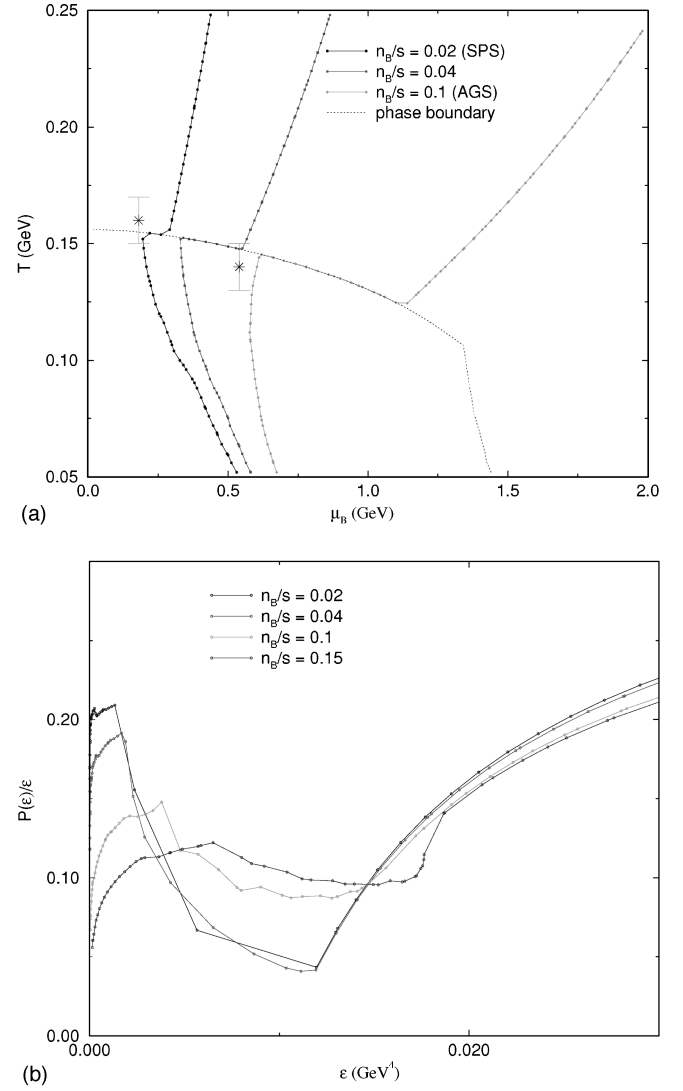


FIG. 3. (a) Paths in the T - μ plane for different baryon admixtures, for resonance gas plus the QGP; (b) the ratio of pressure to energy density, p/ϵ , versus ϵ , for different baryon admixtures.

$$\begin{aligned} s^{\text{excl}}(T, \{\mu_i\}) &= \left(\frac{\partial P^{\text{excl}}}{\partial T} \right)_{\{\mu_i\}} = \frac{\sum_j s_j^{\text{ideal}}(T, \tilde{\mu}_j)}{1 + V_0 \sum_j n_j^{\text{ideal}}(T, \tilde{\mu}_j)}, \\ \epsilon^{\text{excl}}(T, \{\mu_i\}) &= T s^{\text{excl}}(T, \{\mu_i\}) - P^{\text{excl}}(T, \{\mu_i\}) \\ &\quad + \sum_j \mu_j n_j^{\text{excl}}(T, \{\mu_i\}) \\ &= \frac{\epsilon^{\text{ideal}}(T, \tilde{\mu}_i)}{1 + V_0 \sum_j n_j^{\text{ideal}}(T, \tilde{\mu}_j)}, \end{aligned}$$

and the excluded volume radius $r_0 = 0.7$ fm. We do it just for completeness of the phase diagram: however, we have to stress that all our results are completely independent of what is happening in this corner of the T, μ_b phase diagram, since all the paths we discuss (see below) are far from it.

Apart from the excluded volume factor in p (which is also $\ln Z$), we use standard thermodynamical formulas for the ideal gas of hadrons, stable, and resonances. We use all reso-

nances with $m < 2$ GeV. All other variables are obtained from the pressure $p(T, \mu)$ by standard thermodynamical relations.

C. Adiabatic paths in the phase diagram and the resulting EOS

Although the T - μ plane is rather convenient for the determination of the thermodynamical parameters in both phases, the mixed phase domain is hidden behind the transition line. As is well known, in the mixed phase a new thermodynamical variable is the fraction f of the volume occupied by the QGP phase. Besides, as we will show shortly, the cooling trajectory in the T - μ plane is rather complicated.

If the expansion of matter¹³ is slow enough, the *entropy is conserved*. We assume it in what follows. If so, the conjugates to the (T, μ_b) pair—the entropy s and the baryon density n_b —provide a more natural description. If those variables are used, the cooling paths would be just straight lines, going from the initial point toward the origin. As the entropy per baryon ratio stays constant, the paths can be marked by this ratio.

For the EOS described above (the *resonance gas* for the hadronic phase is supplemented by a simple bag-type quark-gluon plasma) we have calculated those paths in all variables. In Fig. 3(a) we show what these paths look like on the original phase diagram. The lines are marked by the n_b/s ratio. Those for $n_b/s = 0.02, 0.1$ correspond approximately to SPS (160 GeV nucleon) and AGS (11 GeV nucleon) heavy ion collisions, respectively. Note that the trajectory has a nontrivial zigzag shape,¹⁴ with reheating in the mixed phase. The end point of the QGP branch was named [32] the “softest point,” while the beginning of the hadronic one can be called the “hottest point.”¹⁵

The next step is to define the effective EOS in the form $p(\epsilon)$ (needed for hydrodynamics) *on these lines*: that is shown in Fig. 3(b). Note that the QCD resonance gas in fact has a very simple EOS¹⁶ $p/\epsilon \approx \text{const}$, while displaying a strong dive toward the minimum of p/ϵ (the “softest point”). The contrast between “softness” of matter at dense stages and relative “stiffness” at the dilute ones is strongly enhanced for the SPS case: it is the main physical phenomenon we study below.

For comparison, one should also look at the (effective) EOS corresponding to popular cascade event generators. For RQMD (with repulsive potential between baryons) it was studied in a recent work [16] for AGS energies. A rather simple EOS was found, about the same for the compression

and expansion stages. For (transverse) pressure and energy density it is approximately $p/\epsilon \approx 0.14$. It is very close to what our resonance gas gives for the corresponding s/n_b ratio. (It would be nice to have similar results for other cascades, and in a wider energy range.)

In summary, resonance gas (even with baryons) has a very simple EOS, $p/\epsilon \approx \text{const}(\epsilon)$. However, lattice results (modeled via a bag-type model for QGP) indicate that the EOS of hadronic matter is much *softer*, with a small p/ϵ in the interval of the energy densities near the end of the mixed phase.

IV. HYDRODYNAMICS

The equations of relativistic hydrodynamics are standard:

$$\partial_\mu T_{\mu\nu} = 0, \quad \partial_\mu n_b u_\mu = 0. \quad (3)$$

In the absence of any dissipative terms, they imply conservation of the entropy $\partial_\mu s u_\mu = 0$ and baryon number N_b . The ratio of their local densities, n_b/s , is not changing, and that is why in our discussion of the thermodynamics above we have parametrized by it the paths on the phase diagram (e.g., T, μ_b). Furthermore, we have shown that hydrodynamics-relevant form of the EOS, namely, $p(\epsilon)/\epsilon$, depends smoothly on this ratio.

It was shown many times (see, e.g., a recent review [29]) that,¹⁷ for PbPb and AuAu collisions at SPS and AGS energies the rapidity spectra of π, K, N, d can be described by some *common* collective motion, convoluted with a thermal one (and this is certainly different for π, K, N, d). It suggests that all matter elements have about the same composition (n_b/s).

As was explained in the previous section, the n_b/s ratio is conserved for each matter element. However, if initial conditions have different n_b/s in different places, it becomes space and time dependent due to flow. Phenomenological observations mentioned in the previous paragraph imply that we may in fact significantly simplify the problem, assuming “well-mixed” initial conditions which have a constant n_b/s everywhere. If so, the equations for baryon flow and entropy flow become the same, and the n_b/s ratio is space-time independent. In practice, one can determine n_b/s from the baryon/meson ratio at the freeze-out stage. We use the values $n_b/s = 0.02$ and 0.085 as representative for SPS (160 GeV nucleon) and AGS (11 GeV nucleon) heavy ion collisions, respectively. These paths corresponding to them on the T - μ plot are also shown in Fig. 3(a).

The initial geometry of the fireball was chosen to be Saxon-like with natural Lorentz contraction in the longitudinal direction. In this work we have not even attempted to discuss the kinetics at the formation stage, and simply adopt a phenomenological approach, introducing the initial longitudinal size z_0 and velocity $v_z = v_0 \tanh(z/z_0)$ as phenomenological

¹³Note that we do not discuss the compression stage here: it is not slow and therefore entropy is in fact produced here.

¹⁴As far as we found, such a shape first appeared in the literature in [12].

¹⁵Of course, in the “Hagedorn sense,” as the hottest point of the hadronic phase.

¹⁶The main difference between the curves with various n_b/s is at the low energy density side: obviously adding baryons one contributes much more to the energy density than to pressure. As we will show below, it will have a significant impact on the mean radial flow.

¹⁷For clarity, this statements holds for central collisions of heavy enough ions, which have a very small “corona” of punched through nucleons. For medium and light ions it is obviously more visible, and asymmetric systems have many spectator nucleons. Certainly those are not part of the hydrodynamics fireball.

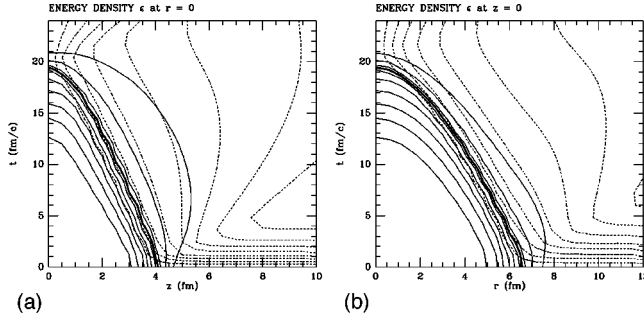


FIG. 4. Hydrodynamical solution for 11.6 A GeV Au+Au. The solid contours are energy density contours, with one bold contour being the boundary between the mixed and hadronic phases ($\epsilon = 0.35$ GeV/fm³). The dotted contours are the longitudinal (left) and radial (right) velocity contours, corresponding to velocity values of 0.01, 0.05, 0.1, 0.2, 0.3, 0.4, and 0.5 from left to right.

parameters. As a result, we do not have a predictive power as far as the rapidity distribution is concerned, but we can just fit it (as was done many times before; see [9]). We concentrate below on the central region of the rapidity, and do not intend to describe well spectra in the target or projectile fragmentation region. Although we describe most of the secondaries, the total energy of the hydrodynamics subsystem is only a fraction of the total one. For 160A GeV Pb+Pb the total initial energy of the hydrodynamical system is about 0.4 of the total center-of-mass collision energy (which corresponds to an initial central energy density of 4 GeV/fm³), while for 11.6A GeV Au+Au this ratio (the *inelasticity coefficient*) is about 0.7 (which corresponds to an initial central energy density of 1 GeV/fm³).

The uncertain *initial conditions* are not important for transverse flow, because it is accumulated over a long time. We will return to a discussion of hydrodynamics and radial flow results later, after we study the kinetics of freeze-out in more details.

A typical solution for 11.6A GeV Au+Au is shown in Fig. 4 while for 160A GeV Pb+Pb it is shown in Fig. 5. Let us make a few comments about them. First of all, they are qualitatively different. While at the former (AGS) energy the longitudinal and transverse expansion are not that different, at SPS ones the *longitudinal* flow has already distinct ultrarelativistic (Bjorken-like) features, with most isotherms being close to hyperbolas, the lines of constant proper time

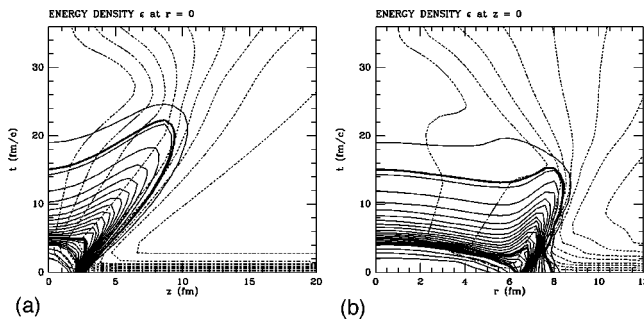


FIG. 5. Hydrodynamical solution for 160A GeV Pb+Pb. Notation is as in the previous figure; only now there are two bold contours, being the mixed-hadronic and quark-mixed boundaries with energy densities $\epsilon=0.18$ and 1.4 GeV/fm³, respectively.

$\tau = \sqrt{t^2 - z^2}$. What is less obvious (and follows from a particular EOS including the QCD phase transition) is also a dramatic difference in the *transverse* flow at AGS and SPS as well. The former can be described as “burning in”; the lines of constant energy density move inward with some small constant speed. At SPS the mixed phase matter burns into the low density hadron gas at a “burning log,” which is nearly time independent and positioned at a transverse radius of 6–8 fm. With time, as more matter flows from the center, there is even a tendency to get by the end of the expansion a hole at $r=0$, with less density there than in the “burning log” region. Such behavior is a result of overshooting the “softest point” in the initial conditions, and it is even more dramatic at higher (RHIC and LHC) energies; see [33].

(It is interesting to note that our hydrodynamics solutions in many cases show late *implosion*, with subsequent secondary explosion from the center $r=0$. However, it is happening well after freeze-out. Such a hydrodynamics solution can only become physical if colliding nuclei are much larger than the heaviest existing ones.)

V. KINETICS OF FREEZE-OUT

Although there is rather substantial theoretical literature related to the kinetics of freeze-out, and all major concepts (and most of the details) to be used below have been developed before, in most of the previous hydrodynamical models freeze-out is formulated in a very crude, oversimplified form. Most of them simply assume that all reactions stop when the system reaches some *universal* “final temperature” $T_f \approx 140$ MeV. However, this approximation is clearly inadequate since (i) different processes have different rates, say, inelastic and elastic ones, (ii) different secondaries have different rates, (iii) the expansion rates are very different for different colliding nuclei, and even for the same nuclei for different matter elements.

To learn more about freeze-out conditions and resolve the issue phenomenologically, one can study various observables, such as HBT radii, deuteron production, Coulomb effects [20], event-per-event fluctuations [42], the pion chemical potential, etc. Except for the last one, we do not so far have HKM predictions for them, and leave those for studies elsewhere.

A. Local freeze-out conditions

The central point we would like to make is as follows. Although each individual matter element follows roughly the same path on the phase diagram, the relevant kinetics is *not* the same because they move along these paths with different speeds. In particular, freeze-out happens at higher T, μ when the time evolution is faster (smaller initial system or closer to the edge of the system) relative to matter elements for which the evolution is slower. Accounting for it turns out to be crucial for applications we have in mind in this work.

Fortunately, after the global collective motion of matter is already determined from hydrodynamics calculations, we know the expansion rate of any matter element at any time. With this information at hand, plus the known kinetics of various hadronic processes, we can formulate realistic conditions under which subsequent *freeze-outs* (decoupling of a

particular reaction) take place.

The principle idea of a freeze-out goes back to the famous 1951 Pomeranchuk paper (which initiated Landau to suggest a hydrodynamics-based approach for the first time). The condition Pomeranchuk had in mind is a relation between the mean free path and the system dimensions. The particular form we use (as far as we know, mentioned first in [30] and used in real hydrodynamics in [31]) is based on a similar condition, which is, however, a *local* (or differential) value of the ratio¹⁸

$$\xi = \tau_{\text{expt}} / \tau_{\text{coll}} \quad (4)$$

where $1/\tau_{\text{coll}}$ is the collision rate per particle considered per unit proper time. The invariant expression for the expansion time can be given in terms of the four-velocity u_μ of the flow,

$$1/\tau_{\text{expt}} = \partial_\mu u_\mu. \quad (5)$$

Hydrodynamics is applicable (the dissipative terms are small) when $\xi \gg 1$, while if $\xi \ll 1$, the reactions in question can be ignored. The boundary at which $\xi \sim 1$ exists both at the formation and expansion stages, forming some three-surface around the four-volume in which hydrodynamics is applicable. Furthermore, in principle the situation is more complicated, with ξ large and small for different variables.

First of all, let us distinguish two classes of reactions: (i) the inelastic reactions leading to the creation or annihilation of a certain species of particles and (ii) elastic rescatterings leading to simple momentum exchange. It is well known that the former need higher collision energies than the latter. (For example, in a gas of massless pions one can use chiral perturbation theory to evaluate reaction rates, and pion production depends on temperature as $1/\tau_{\text{production}} \sim T^9$ while elastic rescattering is $1/\tau_{\text{rescattering}} \sim T^5$. Clearly, as the expansion cools the gas, their decoupling happens at different points.) Separating those two classes, one usually defines *chemical* and *thermal* freeze-out, for these two classes of reactions. The second important point is that both freeze-outs should be determined for *each* species separately.

For chemical freeze-out this distinction, however, is not very important in practice, since in fact all reactions changing particle composition can be seen to be rather ineffective during the hadronic phase, for all AGS and SPS collisions.¹⁹ In QGP (most) hadrons do not exist at all, and thus the natural place for ‘‘hadronization’’ is what we call the mixed phase. How it happens remains unknown, but there are rather convincing arguments that it happens rapidly enough. Those are based on quite extensive work on a thermal description of many hadronic species [35,27], mainly in connection with the so-called ‘‘strangeness enhancement’’ phenomenon. It

was found that (within the existing experimental uncertainties, not always small) one can describe most of the particle ratios in a thermal model. The resulting values for T and μ_b are shown in Fig. 3 as two crosses, for the AGS and SPS energies, respectively. Both are close to the ‘‘hottest points’’ of the corresponding paths: this is consistent with the idea that chemical equilibration cannot indeed be kept in the hadronic gas phase.

We have built in this idea into the HKM: any ‘‘hadronic chemistry’’ in the hadronic phase is ignored. It is assumed that it ends together with hadronization, and when the path departs from the phase transition line T_c, μ_c no more changes in particle composition (apart from resonance decays) are included. Therefore our particle composition is exactly the same as in the thermal model [27] (which has thermodynamics of exactly the same resonance gas with excluded volume). We therefore do not duplicate the tables for particle ratios here, referring the interested reader to this work.

B. Between chemical and thermal freeze-out

We do not provide an extensive introduction for this section: for a good overview and references see [41]. Switching off all reactions changing the particle composition, we have made *any* particle number N_i to be a conserved quantity. The point is simply that at this stage of the evolution one has to introduce chemical potentials for all particle species,²⁰ μ_i . Their values are then determined by those predetermined values of N_i in the usual way. This is in contrast to chemical equilibrium, in which most of them are zero, and only chemical potentials conjugated to conserved quantities (baryon charge and strangeness) were needed.

It is instructive to see how, as one starts with a chemically equilibrated hadron gas with $\mu_i = 0$, the nonzero values appear as the system cools further.²¹ The thermodynamical relation written in the form

$$(\epsilon + p)/nT - s/n = \mu/T \quad (6)$$

is especially useful. For slow (adiabatic) expansion the s/n ratio is not changing, while in the first term on the left-hand side (LHS) the chemical potential *nearly* cancels (it does exactly provided a Boltzmann approximation is used). So one can read the T -dependence of μ directly from the RHS. The notorious exceptional case worth mentioning is that for massless particles, for which the whole LHS is just a con-

¹⁸The nonlocal condition in line with the original Pomeranchuk idea is worked out in [45], but we feel it is still way too complicated to use in practice in the hydrodynamics context, because of the integrals toward future propagation involved.

¹⁹For example, for strangeness production reactions this statement was well documented long ago; see [34].

²⁰For clarity, those potentials are conjugated to the total number of particles, and so, say, for pions they enter distributions of π^+ , π^- , π^0 with the same sign.

²¹To our knowledge, it was first pointed out in the context of the pion gas by Baym (private communication). Further discussion of this idea and of the kinetics of the pion gas can be found in [36], mostly in relation to the question of the possible evolution of the nonzero chemical potential for the pions. For a discussion of the *opposite* scenario, suggesting overpopulation and a large positive chemical potential for pions already at this point, see [37].

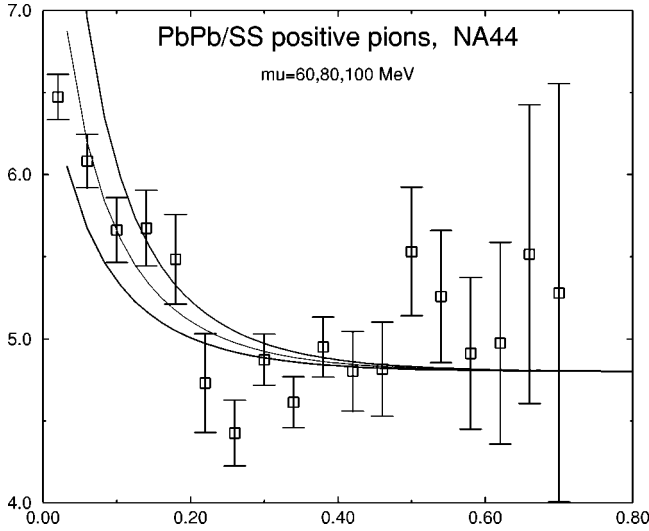


FIG. 6. The ratio of π^+ p_t spectra for PbPb and SS collisions versus p_t (in GeV). Points are NA44 experimental data; three curves correspond to the pion chemical potential $\mu_\pi = 60, 80,$ and 100 MeV (from bottom up).

stant. Therefore $\mu/T = \text{const}$, and so if $\mu = 0$ at the beginning, it remains so for any T .²²

Accounting for the nonzero pion mass and Bose statistics one finds $\mu_\pi(T)$; see [42]. For example, if one assumes that $\mu_\pi(T_c = 160 \text{ MeV}) = 0$, one finds that by a thermal freeze-out (which happens for PbPb collisions at CERN at $T = 110\text{--}120$ MeV) the pion chemical potential $\mu_\pi = 60\text{--}80$ MeV.

In order to see whether such an effect really occurs in experiment, we have plotted in Fig. 6 the ratio of the p_t spectra for PbPb collisions (in which we expect thermal freeze-out at $T = 100\text{--}120$ MeV, and thus the formation of a significant pion chemical potential) to our reference point, central SS collisions (for which the effect should be much smaller). The data sets are both for *positive* pions²³ from an NA44 experiment [5], in the same experimental settings (and thus systematic errors should somewhat cancel). One finds that there is significant enhancement of this ratio at small p_t , which agrees with the formation of the nonzero pion chemical potential. Moreover, as one can see, the magnitude of the effect is in approximate agreement with our estimates.

(Additional comments: PbPb and SS collisions have a somewhat different stopping of baryons. For *positive* pions an extra stopped charge for PbPb would decrease low p_t pion production due to the Coulomb field, contrary to observations. Another effect that contributes in the opposite direction is feeding to low p_t pions from extra Δ decays coming from extra baryons in PbPb as compared to SS. The magnitude of those effects is comparable, and thus they may cancel out to some extent.)

The secondaries other than pions can be to a good accuracy treated as a Boltzmann nonrelativistic gas, and so one

can easily derive the following relation between the chemical potentials at chemical and thermal freeze-out:

$$\mu_{\text{th}} = \mu_{\text{ch}} \frac{T_{\text{th}}}{T_{\text{ch}}} + m \left(1 - \frac{T_{\text{th}}}{T_{\text{ch}}} \right). \quad (7)$$

(In particular, for very large systems $T_{\text{th}} \rightarrow 0$, the chemical potential $\mu_{\text{th}} \rightarrow m$ as it should, and one can then proceed to normal nonrelativistic notation.) When implemented in the HKM, this relation ensures that the particle ratios are *independent* of any details of the thermal decoupling we discuss below.

C. Thermal freeze-out for different species

Now we are in the position to discuss particular reactions in the resonance gas. Rather extensive studies have been made in the past; see [43]. Let us start with qualitative comments first.

Out of the many reactions which include pions the major processes are the low energy elastic $\pi\pi$, πK , and πN scattering. Those have an especially large cross section due to the existence of the low energy resonances ρ , K^* , and Δ , respectively.

Estimates of the $\pi\pi$ collision rate using the chiral Lagrangian were made by one of us [38] and, in more detail, in Ref. [39]. The result

$$1/\tau_{\pi\pi} = T^5 / (12F_\pi^4) \quad (8)$$

(where F_π is the pion decay constant, 93 MeV) displays a very strong T dependence. This feature remains true when one includes the resonances [41]: basically in the interval we deal with ($T = 120\text{--}150$ MeV) the pion-pion scattering rate increases by a factor of 2.²⁴ These rates are increased further by the inclusion of the nonzero value of the pion chemical potential discussed in the preceding subsection.

A strong T dependence leads to the following qualitative feature of freeze-out: relatively modest changes in the freeze-out temperature correspond to quite significant changes in the duration of the collision-dominated (hydrodynamics) expansion. As we will see below, this will translate into significantly stronger flow.

The πN cross section is very large, reaching about 200 mb at the Δ resonance peak. The naive radius of the interaction $R = \sqrt{\sigma/\pi} \approx 2.6$ fm is so large that one may question simple cascades and think about collective effects (“pibars”). Absolute scattering rates depend on the density of nucleons at the decoupling stage. At AGS the (isospin-averaged) rate is of the order of $1/\tau_{\pi N} \approx 100$ MeV, which is larger than $1/\tau_{\pi\pi}$. Since the nucleon to pion ratio is about 1, the rates are very close also. At SPS energies the situation is quite different: the nucleon/pion ratio is about 1/5. It makes

²²This is what happens in the case of background radiation in an expanding universe: photons do not collide after the big bang, but they still have the Planck spectrum, with $\mu = 0$.

²³The π^-/π^+ ratio shows a larger enhancement, which is known to be due to Coulomb effects; see e.g., [20].

²⁴Furthermore, the inclusion of resonances changes the dependence on the pion momentum p : in contrast to the chiral result the rate becomes basically flat for $p < 700$ MeV we need, and decreases for larger p (now, in contrast to the lowest order chiral result which predicts an unphysical rise with p).

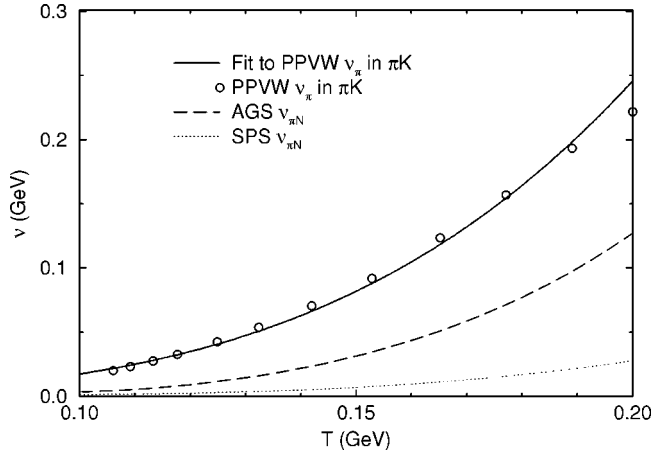


FIG. 7. Pion collision rates $\nu = \tau_{\text{coll}}^{-1}$ [GeV] in a pion-kaon-nucleon gas versus temperature T [GeV]. PPVW stands for Prakash, Prakash, Venugopalan, and Welke.

the πN scattering less important for pions, but nucleons have a very large collision rate and thus should freeze out very late. Kaons and other strange secondaries have smaller collision rates.

We have already mentioned a special case of ϕ with the scattering and absorption cross sections in the few mb range. Clearly one can completely ignore their rescattering in the hadronic phase: we assume therefore that their thermal freeze-out (as well as chemical one) coincides with the end of the mixed phase.

Let us now provide more quantitative information about the rates we use (see also [43]). The general formula for the averaged collision rate of particle a resulting from a binary collision with particle b is given by

$$\Gamma_{ab}^a(T) = \int \frac{d^3\mathbf{p}_a}{(2\pi)^3} \frac{d^3\mathbf{p}_b}{(2\pi)^3} \frac{1}{e^{E_a/T \pm 1}} \frac{g_b}{e^{E_b/T \pm 1}} \sigma_{ab} \times [(p_a + p_b)^2] \left| \frac{\mathbf{p}_a}{E_a} - \frac{\mathbf{p}_b}{E_b} \right| \bigg/ \int \frac{d^3\mathbf{p}_a}{(2\pi)^3} \frac{1}{e^{E_a/T \pm 1}}, \quad (9)$$

where E_a is the energy of a (minus any chemical potential

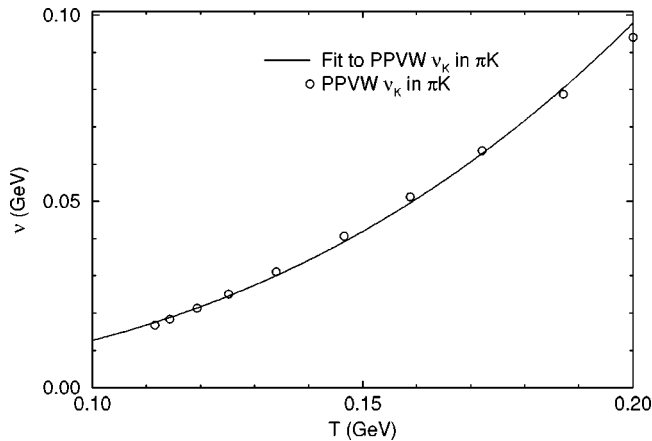


FIG. 8. Kaon collision rates.

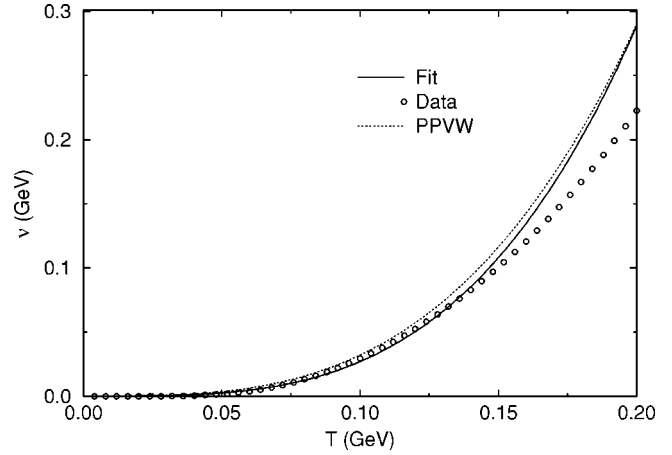


FIG. 9. Nucleon collision rates. ‘‘Data’’ refers to numerical integration of the cross sections, as described in the text. The curves marked ‘‘fit’’ refers to a fit using the data points below 0.15 GeV, which is used in the HKM for the determination of the freeze-out surface.

for E_a within the thermal exponent), and similarly for b . g_b is the multiplicity of b and the sign in the denominator of the thermal weights is chosen based on whether a, b are a fermion or boson. For example, for the πN rate we take the $\pi^+ p$ total cross section from the Particle Data Group [44] and notice that by isospin arguments, the averaged πN cross section is

$$\sigma_{\pi N}^\pi \simeq \frac{2}{3} \sigma_{\pi^+ p} \quad (10)$$

and the pion collision rate due to πN scattering is

$$\Gamma_{\pi N}^\pi(T) = \int \frac{d^3\mathbf{p}_\pi}{(2\pi)^3} \int \frac{d^3\mathbf{p}_N}{(2\pi)^3} \frac{1}{e^{E_\pi/T - 1}} \frac{4/3}{e^{(E_N - \mu_b)/T + 1}} \sigma_{\pi^+ p} \times [(p_\pi + p_N)^2] \left| \frac{\mathbf{p}_\pi}{E_\pi} - \frac{\mathbf{p}_N}{E_N} \right| \bigg/ \int \frac{d^3\mathbf{p}_\pi}{(2\pi)^3} \frac{1}{e^{E_\pi/T - 1}}. \quad (11)$$

Using $\mu_b(T)$ from the previous section we can evaluate the above integral numerically. The results are shown in Fig. 7, for the $\pi\pi, \pi K$ rates combined (dots and fitted curve) and for its πN component at AGS and SPS. The total pion collision time is then given by

$$\tau_{\text{collision}}(T) = [\Gamma_{\pi\pi}^\pi(T) + \Gamma_{\pi N}^\pi(T)]^{-1}. \quad (12)$$

For kaons we simply take the πK rate from [43] which we show in Fig. 8. We have ignored smaller KN collision rates: therefore (as also noted in [43]) we do not distinguish the rates for kaons and antikaons.

For nucleons, the πN interaction is the dominant process [43] and we have the expression

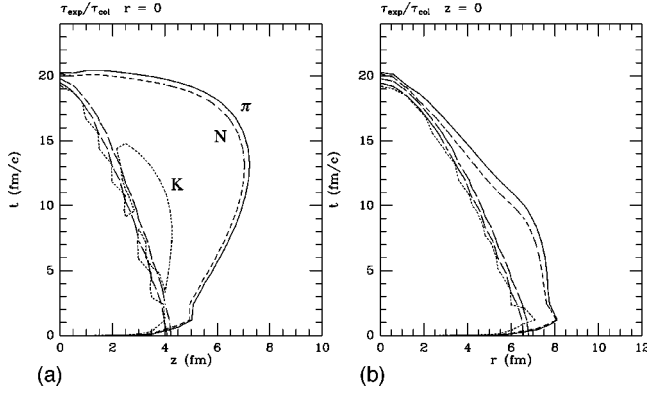


FIG. 10. Freeze-out surfaces for 11.6A GeV Au+Au. The solid line corresponds to pions, the dashed to nucleons, and the dotted one to kaons. The two long-dashed curves indicate two isotherms, with $T=160$ (the lower curve, at critical T) and 140 MeV.

$$\Gamma_{\pi N}^N(T)$$

$$\begin{aligned} &= \int \frac{d^3 \mathbf{p}_N}{(2\pi)^3} \int \frac{d^3 \mathbf{p}_\pi}{(2\pi)^3} \frac{2}{e^{E_\pi/T} - 1} \frac{1}{e^{(E_N - \mu_b)/T} + 1} \sigma_{\pi^+ p} \\ &\times [(p_\pi + p_N)^2] \left| \frac{\mathbf{p}_\pi}{E_\pi} - \frac{\mathbf{p}_N}{E_N} \right| \int \frac{d^3 \mathbf{p}_N}{(2\pi)^3} \frac{1}{e^{(E_N - \mu_b)/T} + 1} \end{aligned} \quad (13)$$

noting that $g_\pi = 3$. It turns out that due to the almost factorizable nucleon density inside the main integral, the effect of μ_b is almost negligible. In Fig. 9 we present the common rate for the AGS and SPS and compare with the SPS nucleon rate from [43].

The remaining issue is what value of the ratio in the condition (4) one should use in order to optimize the surface. Consider for example the simplest case in which reactions proceed at later times with the rates $dn/dt = (1/\tau_{\text{coll}}) \exp(-t/\tau_{\text{exp}})$. Integrating this rate from $\tau=0$ to infinity one gets the number of collisions left over to be ξ . As we want to cut roughly in the middle of the last collision, one may think the optimal point is close to $\xi=1/2$. Our checks with cascades (see below) confirm this choice, although one may in the future improve on this point.

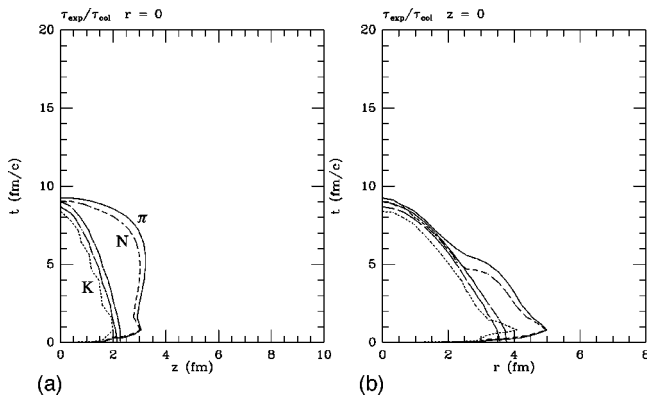


FIG. 11. Freeze-out surfaces for 14.6A GeV Si+Al: notation is the same as in the previous figure.

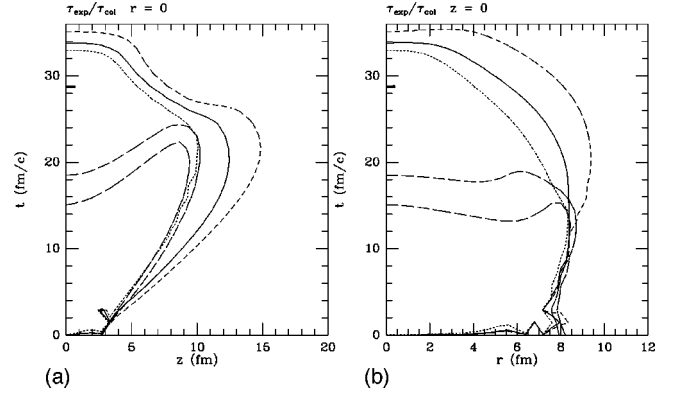


FIG. 12. Freeze-out surfaces for 160A GeV Pb+Pb.

Using these rates and the condition (4), we determine the freeze-out three-dimensional (3D) surface. Several representative cases are shown in Figs. 10–13, shown as a section by time–longitudinal-coordinate (t - z) plane (at transverse coordinate $r=0$) and the t - r plane ($z=0$). We have already commented on the dependence on the particle kind above. Note also the significant difference between heavy and light ions. As expected, one finds that the larger the system is, the lower T_{th} is on this surface.

Furthermore, the shape of the freeze-out surface is very different from simple isotherms. It means that there is a significant variation of this temperature over the surface itself: in order to find the coolest pion gas, one should look at the very center of central collisions of heaviest nuclei at highest available energy.

Finally, after elements of the freeze-out surface are determined (from the hydrodynamics solution plus kinetic condition discussed above) by (3D) triangularization (see the Appendix), the HKM program generates secondaries using the Cooper-Frye formula²⁵

$$E \frac{dN}{d^3 \mathbf{p}} = \frac{1}{(2\pi)^3} \int \frac{p^\mu d\sigma_\mu}{e^{p \cdot u/T \pm 1}}, \quad (14)$$

where the integral is taken over the freeze-out surface, with $T_{\text{th}}, \mu_{\text{th}}, u_\mu$ changing from point to point.

The last step of the HKM is the decay of all resonances (and weak decays of stable particles, if needed) into the final secondaries. The standard output, as from other event generators, includes information about particle momenta, the time and place of their production, and the parent resonance (if they come from a decay).

The particular formulation of the model outlined above can of course be further questioned and refined. In particular, since different species of particles have different freeze-out surfaces, one get intermediate regions in which part of them

²⁵Although this formula is conserving energy and is widely used, there is still a well-known problem with it when applied to the *spacelike* part of the freeze-out surface: it includes also particles which move toward the excited system, which would be reabsorbed. Possible improvements are discussed, e.g., in recent work [19]: we have not included those in the HKM.

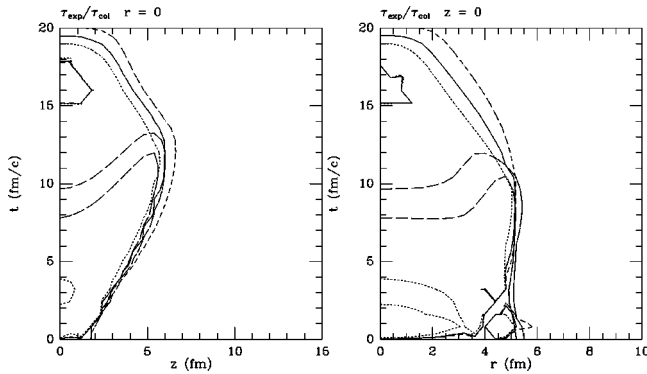


FIG. 13. Freeze-out surfaces for 200A GeV S+S.

are already in a free-streaming regime and part still interacting. In principle, one should modify the EOS for that effect.

Note, however, that the free-streaming particles of one kind (e.g., pions) continue to interact with other kinds (e.g., nucleons). In particular, we already commented above that at SPS there are much more pions than nucleons: therefore, even with the πN cross section being the dominant one, the *average* pion decouples earlier than the *average* nucleon. But even then the ‘‘pion wind’’ continues to blow and accelerates the nucleons, contributing to the nucleon flow. Thermal freeze-out does not change the pion number: the only difference (which we have ignored) is a somewhat different momentum distribution of the free-streaming and the interacting pion ensembles.

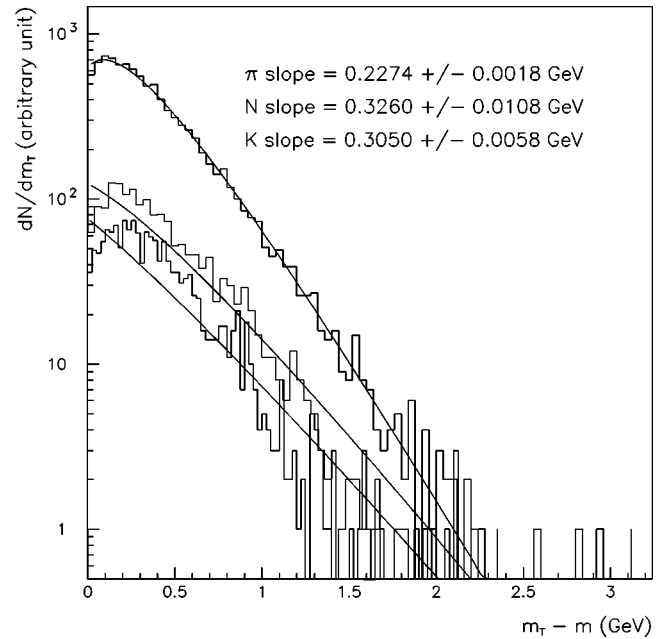
VI. FURTHER HYDRODYNAMICS RESULTS: THE RADIAL FLOW

In the previous section we have shown that the improved thermal freeze-out condition leads to a huge difference compared with simple isotherms. For the same fixed value of $\tau_{\text{expt}}/\tau_{\text{coll}}$ one gets very different conditions for different A , also for large and small y (the central region cools further). These observations provide natural resolutions to the puzzling observations related to strong A and y dependence of the flow discussed above.

The key point here is as follows: although these modifications do not significantly prolong the total lifetime, they significantly increase the lifetime of the hadronic phase. It is important for flow, because it is the part of the evolution path at which the matter is most ‘‘stiff’’ (has a larger p/ϵ). Thus improved freeze-out leads to a significant ‘‘extra push,’’ and explains strong flow.

The typical p_t spectra for π, K, N we obtain (after resonance decays) are shown in Fig. 14(a), together with their fixed-slope fits.

In Figs. 15 and 16 we show the distribution over transverse velocities calculated over all matter elements on the freeze-out surfaces. We show only heavy ions, for AGS and SPS energies. The distributions always have a sharp peak at their right end, which is more pronounced at SPS. Its position depends significantly on the particle type, reaching as high a peak as $v_t=0.6$ for N at SPS. Note the dramatic difference with the isotherms $T=0.14$ GeV which were used in many previous works: for them there is also a peak, but for much smaller $v_t \approx 0.17$, plus a shoulder toward larger

FIG. 14. Typical hydrodynamics output and fit of the m_t distributions for pion, kaon, and protons, for central PbPb collisions at 158 GeV nucleon, at central rapidity $|y| < 0.5$.

values. This difference is much smaller for medium ions (not shown).

In Figs. 17–22 we show how this translates into the observable quantity, the m_t slopes $\bar{T}(y)$. Recall that they include the effect of the freeze-out temperature, flow plus resonance decays, and we show them as a function of rapidity y . We show four cases: AuAu at 11 GeV/nucleon, PbPb at 158 GeV/nucleon, SiAl at 14.6 GeV/nucleon, and SS at 200 GeV/nucleon. In all cases we compare our results with the experimental data available, as well as with the RQMD (which was obtained from standard output files and fitted in the same way as the HKM ones).

For AuAu data at AGS, Fig. 17 one can see that RQMD reproduces slopes very accurately, while our results slightly underpredict the flow. However, it is precisely how it should be, because this version of RQMD has been tuned with a repulsive baryon-induced potential, on the top of the pure

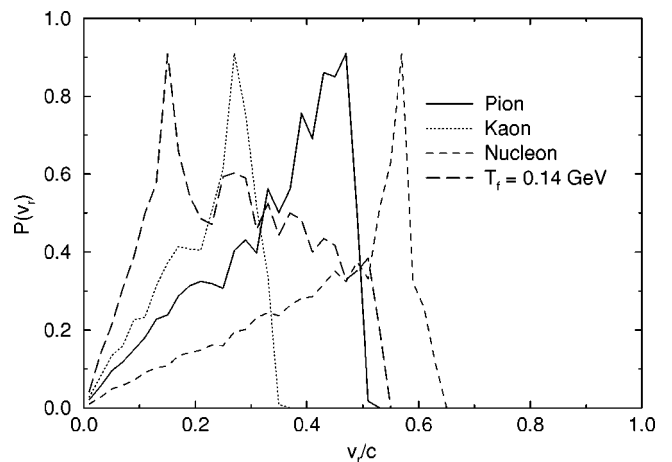


FIG. 15. Transverse velocity distribution over the various freeze-out surfaces for a 160A GeV Pb+Pb collision.

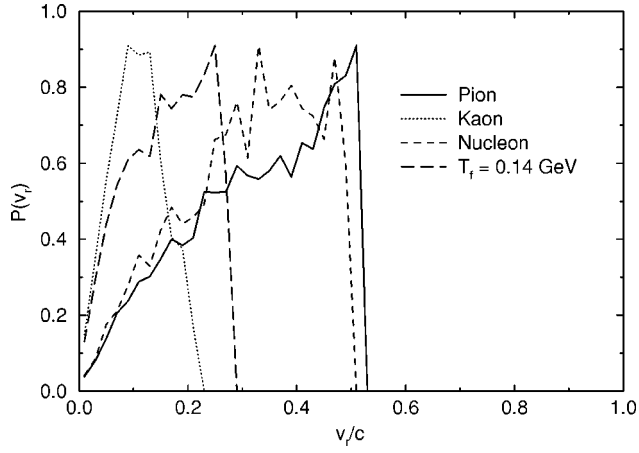


FIG. 16. Transverse velocity distribution over the various freeze-out surfaces for a 1.6A GeV Au+Au collision.

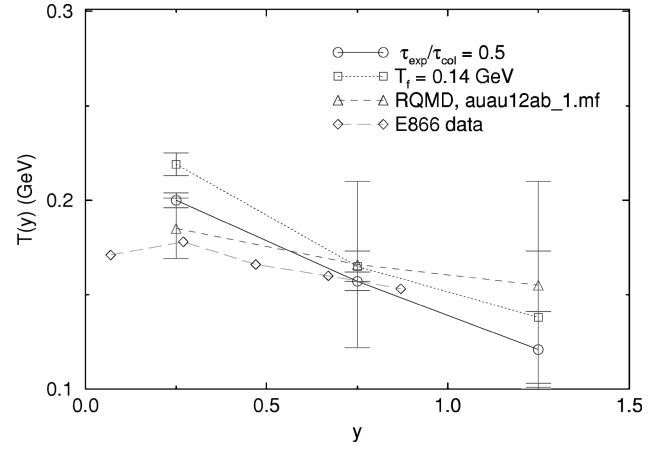


FIG. 19. Kaon slope parameters for 11.6A GeV Au+Au.

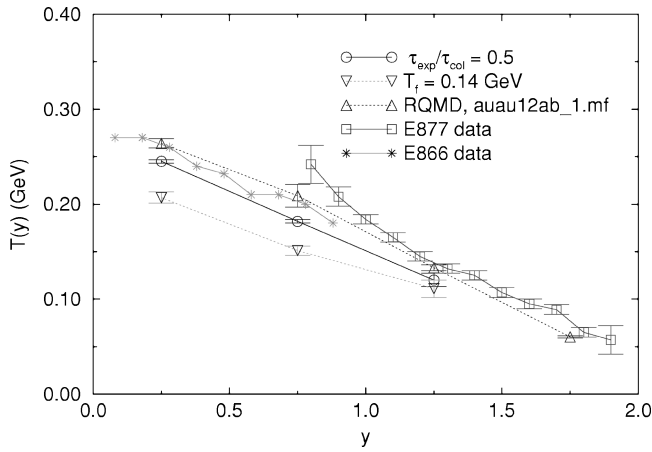


FIG. 17. Nucleon slope parameters for 11.6A GeV Au+Au.

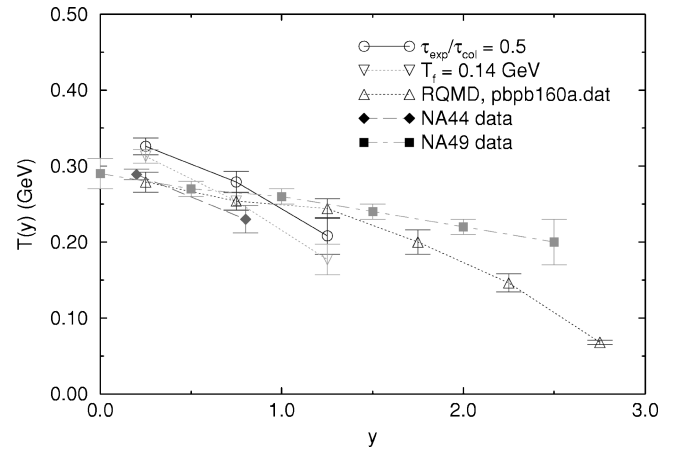


FIG. 20. Nucleon slope parameters for 158A GeV Pb+Pb.

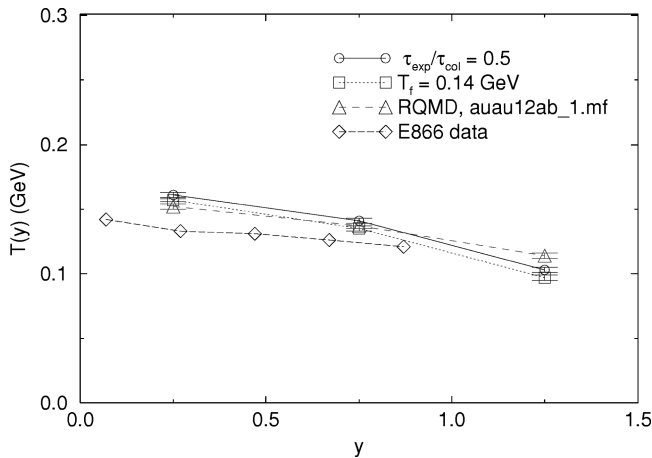


FIG. 18. Pion slope parameters for 11.6A GeV Au+Au.

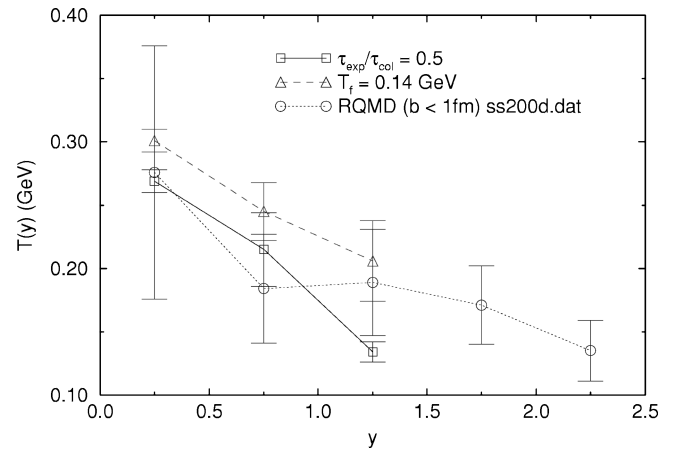


FIG. 21. Nucleon slope parameters for 200A GeV S+S.

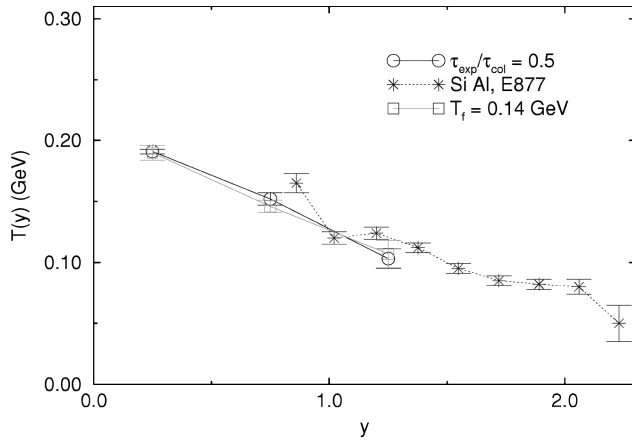


FIG. 22. Nucleon slope parameters for 14.6A GeV Si+Al.

cascade. We have checked that the version without a potential gives a smaller flow, and agrees with our results very well. At the same time, the results following from ‘naive’ freeze-out with $T_f = 140$ MeV are way below.

Figure 20, showing PbPb at 158 GeV/nucleon, looks very similar to Fig. 17. This feature, however, must be a mere coincidence, since both the EOS²⁶ and the space-time picture are quite different. Apart from an obviously rather different longitudinal motion, at AGS the transverse velocity is gained gradually in time (due to about a constant p/ϵ or acceleration, while at SPS our hydrodynamics solution clearly displays the appearance of a ‘burning wall’ regime, at which most of acceleration occurs. Note that nevertheless our results agree with data and RQMD in this case as well, for the same²⁷ $\tau_{\text{expt}}/\tau_{\text{coll}} = 0.5$. This agreement is very nontrivial.

For comparison, let us now discuss lighter ions. An example is shown in Fig. 21, for SS at 200 GeV/nucleon, and one can see from it that our results overpredict the flow in the central region $y \approx 0$. Although for light ions the HKM predicts a shorter lifetime of the hadronic phase and smaller flow [$\tilde{T}_N(y)$ about 30% lower], the data (and RQMD) show that this drop should in fact be larger. It is hardly surprising to see that for medium ions the HKM (and probably hydrodynamics-based models in general) is less accurate.

Let us finally stress that we have not attempted any fine-tuning of the parameters used. The main ingredients, the EOS and freeze-out parameter $\xi = 1/2$, were fixed rather early and not modified when hadron spectra and slopes were calculated. Clearly one can do it and get better agreement. In this work our main objective was to test crudely the systematics of the flow discussed in the Introduction (and, of course, its magnitude).

Finally, a comment on the agreement with RQMD is in order here. We emphasized above that its EOS is similar to ours for the AGS domain, in which both represent the resonance gas, but how can both agree at SPS energies, where our EOS has the notorious softness due to the QCD phase

²⁶Because of the completely different matter composition, the π/N ratio is different by a factor of 5.

²⁷It is also interesting to note that at LBL energies the fit done in [31] prefers the value of this parameter around 0.4, which is not so far from our choice.

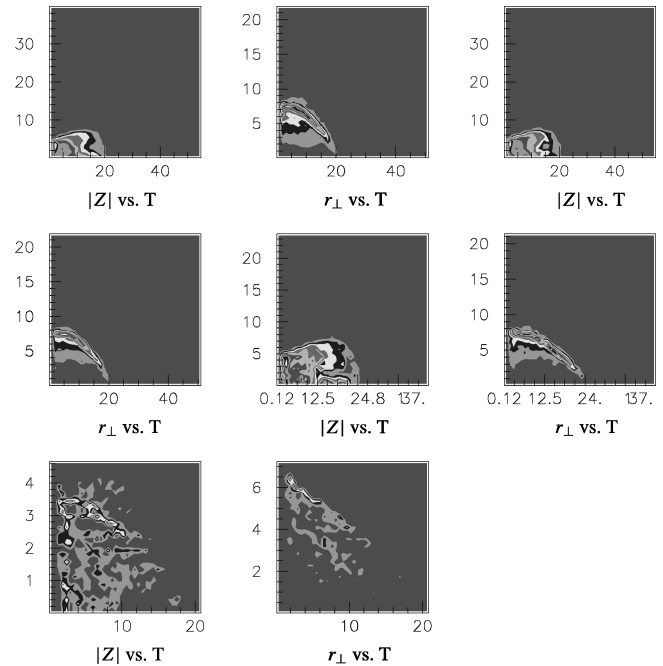


FIG. 23. Space-time distributions for 11.6A GeV Au+Au, hydrodynamics. Eight pictures are projections of the emission points on the z, t and r, t planes, for all secondaries, pions, nucleons, and kaons, subsequently. Resonance decays are included.

transition? In fact, RQMD has its own reasons for changing its EOS to larger ‘softness’: at SPS conditions at early times the energy is stored no longer in resonances, but in (longitudinally stretched) strings. Naturally, those make little pressure in the transverse direction.

By no means do we want to create the impression that our model and RQMD are to a large extent identical. The magnitude and various dependences of the flow we discussed in this work are important observables, but even those give only partial information on the space-time picture of the collision. Looking at these results more closely, one, however, finds significant differences here, which should affect the ‘freeze-out sizes’ extracted by pion interferometry analysis. This statement is illustrated in Figs. 23 and 24, comparing distributions in the points of the last interaction in our model and RQMD. One can see from it that although the average sizes generally agree (and thus flow velocities), their *dispersions* (relevant for interferometry) are rather different. With better data coming, one would be soon able to address this aspect as well.

VII. SUMMARY AND DISCUSSION

In this work we have developed a next-generation hydrokinetic model for heavy ion collisions. Although most of the ideas in it are not new, we believe they are now brought together in an economic and practical way.

Compared to previous hydrodynamics-based models in the literature we have included a number of improvements: (i) a realistic EOS including the QCD phase transition together with the effect of baryons, (ii) a more realistic ‘local’ freeze-out condition, which is based directly on kinetics of rescattering, (iii) the decay of all resonances in the final state, etc.

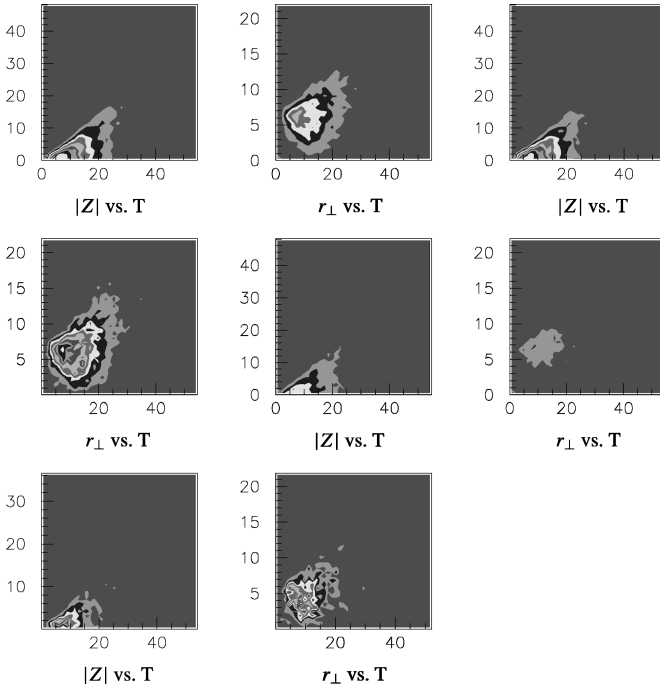


FIG. 24. Same distributions as the previous figure (also 11.6A GeV Au+Au) but for RQMD output file.

Our main focus was on new data on radial flow, including its magnitude, y , A , and s dependence. We have found that our model in general reproduces it well enough. This shows that the lattice-based EOS (which is very soft in the transition region, as we repeatedly emphasized) is in fact consistent with flow data. This is our main result.

The crucial observation which was important for this success is point (ii). It leads to a very simple property of freeze-out: the larger the size of the system is, the cooler the matter at the end becomes. Clearly, deeper cooling for larger A should be seen in many different ways, and we look forward to other ways of testing it.

One may further ask whether data can restrict the EOS. We have not attempted to quantify this in the present work, and only note that for a EOS *without* the QCD phase transition (e.g., a resonance gas, with $p/\epsilon \approx \text{const}$ discussed above) the magnitude of the flow for SPS is indeed too large, and the expansion time too short. Clearly further studies are needed to clarify these issues. A natural extension is discussing 3+1 hydrodynamics at nonzero impact parameters, leading to dipole and elliptic components of the flow.

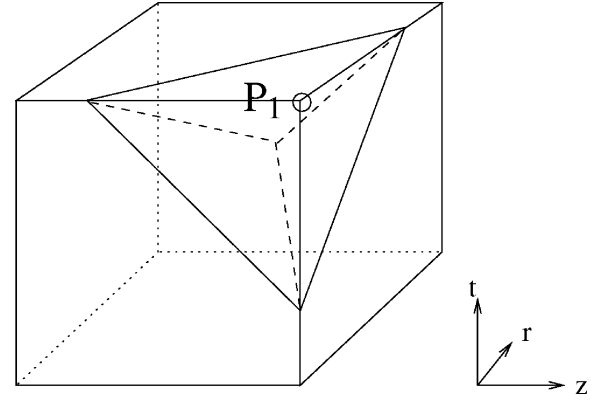


FIG. 25. Triangulation of the freeze-out surface within a single cell. Here P_1 is the only vertex with $\xi > \xi_f$ while all other vertices have $\xi < \xi_f$. This cell will yield three triangles upon triangulation.

Another obvious way to proceed is to calculate the HBT radii and compare it with data. We have already mention that *dispersions* of the emission time and positions in our model are quite different from those resulting from the RQMD.

Clearly only a small fraction of data is considered in this work. To facilitate further use of the model, we plan to deviate from the usual scenario in which only the basics formulas plus *some* results are presented in the paper, and plan to provide the source code and output files, in the same form as event generators do. We hope it will prompt the experimentalist to use it widely, revealing in a wider scope its agreement and disagreement with particular data.

APPENDIX: TRIANGULATION OF THE FREEZE-OUT SURFACE

The surface element on a three-surface of space-time is given by [46]

$$d^3s_\mu = \epsilon_{\mu\alpha\beta\gamma} \frac{\partial x^\alpha}{\partial a} \frac{\partial x^\beta}{\partial b} \frac{\partial x^\gamma}{\partial c} da db dc, \quad (\text{A1})$$

where a, b, c are the coordinates on the three-surface and $\epsilon_{\mu\alpha\beta\gamma}$ is the totally antisymmetric Levi-Civita tensor. For our purposes, because of the cylindrical symmetry of our model, we need to express a finite three-surface element of a freeze-out surface in terms of its corner points. More specifically we want to find d^3s_μ for a triangle defined in (z, r, t) space with corner points (z_i, r_i, t_i) , $i = 1, 2, 3$. It can be shown that, up to a sign,

$$d^3s_\mu = \frac{1}{2} r d\theta \left(\begin{array}{c} \left| \begin{array}{ccc} z_1 & r_1 & 1 \\ z_2 & r_2 & 1 \\ z_3 & r_3 & 1 \end{array} \right|, \left| \begin{array}{ccc} t_1 & z_1 & 1 \\ t_2 & z_2 & 1 \\ t_3 & z_3 & 1 \end{array} \right| \cos\theta, \left| \begin{array}{ccc} t_1 & z_1 & 1 \\ t_2 & z_2 & 1 \\ t_3 & z_3 & 1 \end{array} \right| \sin\theta, \left| \begin{array}{ccc} r_1 & t_1 & 1 \\ r_2 & t_2 & 1 \\ r_3 & t_3 & 1 \end{array} \right| \end{array} \right). \quad (\text{A2})$$

The sign would have to be determined by choosing a direction for the normal of the surface which points outward from the hotter interior of the surface. The output file of the hydrodynamics program gives $(t, z, r, \epsilon, \xi = \tau_{\text{expt}}/\tau_{\text{coll}}, \dots)$ at each point of the output grid [which is typically of size $25 \times 25 \times 25$ in (z, r, t)]. To triangulate the freeze-out surface, we pick a cell and check to see whether ξ (or ϵ if we want a freeze-out surface of constant temperature) on its vertices is

above or below the freeze-out value ξ_f (or ϵ_f). By interpolation we can determine the intersections (if any) between the freeze-out surface and the edges of the cell. Once the intersections are found, we find the center point of these intersection points and connect it to two adjacent intersection points to form a triangle. Continuing this process for all the cells we obtain the desired triangulation of the freeze-out surface (see Fig. 25).

-
- [1] E. Shuryak, Phys. Lett. **78B**, 150 (1978); Sov. J. Nucl. Phys. **28**, 408 (1978).
- [2] T. Matsui and H. Satz, Phys. Lett. B **178**, 416 (1986); D. Kharzeev, and H. Satz, Nucl. Phys. **A590**, 515 (1995); J.-P. Blaizot and J.-Y. Ollitrault, Phys. Rev. Lett. **77**, 1703 (1996).
- [3] CERES Collaboration, G. Agakichev *et al.*, Phys. Rev. Lett. **75**, 1272 (1995); Th. Ulrich, Nucl. Phys. **A610**, 317c (1996); A. Drees, presented at RHIC97, Brookhaven National Laboratory, 1997.
- [4] M. Gonin, NA50 Collaboration, Proceedings of Quark Matter [Nucl. Phys. **A610**, 404c (1996)]; presented at RHIC97, Brookhaven National Laboratory, July 1997.
- [5] I. G. Bearden *et al.*, Phys. Rev. Lett. **78**, 2080 (1997).
- [6] E. V. Shuryak, Sov. J. Nucl. Phys. **20**, 295 (1975); W. Blumel, P. Koch, and U. Heinz, Z. Phys. C **63**, 637 (1994).
- [7] F. Becattini, presented at “Strangeness and Quark Matter 97,” Santorini, Greece, 1997; hep-ph/9708248.
- [8] E. Shuryak and O. V. Zhironov, Phys. Lett. **89B**, 253 (1979).
- [9] D. K. Srivastava, J. Alam, and B. Sinha, Phys. Lett. B **296**, 11 (1992); J. Sollfrank *et al.*, Phys. Rev. C **55**, 392 (1997); B. R. Schlei, U. Ornik, M. Plumer, D. Strottman, and R. M. Weiner “Hydrodynamical analysis of single exclusive spectra and Bose-Einstein correlations,” hep-ph/9509426.
- [10] E. Schnedermann and U. Heinz, Phys. Rev. C **50**, 1675 (1994); T. Csorgo and B. Lorstad, Heavy Ion Phys. **4**, 221 (1996).
- [11] A. Dumitru *et al.*, “Probes for the early reaction dynamics of heavy ion collisions at AGS and SPS,” nucl-th/9705056, (1997).
- [12] P. R. Subramanian, H. Stocker, and W. Greiner, Phys. Lett. B **173**, 486 (1986).
- [13] B. R. Schlei, “Extracting the equation of state of nuclear matter through hydrodynamical analysis,” LA-UR-97-2162, nucl-th/9706037, 1997.
- [14] U. Mayer and U. Heinz, Phys. Rev. C **56**, 439 (1997).
- [15] J.-Y. Ollitrault, Phys. Rev. D **40**, 229 (1992).
- [16] H. Sorge, Phys. Rev. Lett. **78**, 2309 (1997); nucl-th/9610026.
- [17] N. Xu, Nucl. Phys. **A610**, 175c (1996); J. P. Wessels, “Flow phenomena at AGS energies,” nucl-ex/9704004.
- [18] L. D. Landau and S. Z. Belenky Usp. **56**, 309 (1955) [Sov. Phys. Usp. **56**, 309 (1955)]; Nuovo Cimento Suppl. **3**, 15 (1956).
- [19] L. Czernai, Heavy Ion Phys. (to be published).
- [20] H. W. Barz, J. P. Bondorf, J. J. Gaardhoje, and H. Heiselberg, “Freezeout time . . .,” nucl-th/9704045.
- [21] ϕ production in PbPb collisions, NA49 Collaboration home page.
- [22] A. Leonidov, M. Nardi, and H. Satz, Z. Phys. C **74**, 535 (1997).
- [23] E. Laerman Nucl. Phys. **A610**, 1c (1996); T. Schaefer, *ibid.* **A610**, 13c (1996).
- [24] E. Shuryak, “The phases of QCD,” presented at RHIC Summer Study 96, hep-ph/9609249.
- [25] E. Shuryak, Yad. Fiz. **16**, 395 (1972) [Sov. J. Nucl. Phys. **16**, 395 (1972)]; R. Venugopalan and M. Prakash, Nucl. Phys. **A546**, 718 (1992).
- [26] R. Mattiello, A. Jahns, H. Sorge, H. Stoecker, and W. Greiner Phys. Rev. Lett. **74**, 2180 (1995); J. L. Nagle, B. S. Kumar, D. Kusnezov, H. Sorge, and R. Mattiello, Phys. Rev. C **53**, 367 (1996).
- [27] P. Braun-Munzinger and J. Stachel, Nucl. Phys. **A606**, 320 (1996).
- [28] H. Sorge, Phys. Lett. B **373**, 16 (1996),
- [29] J. Stachel, Nucl. Phys. **A610**, 509c (1996).
- [30] J. Bondorf, S. Garpman, and J. Zimanyi Nucl. Phys. **A296**, 320 (1978).
- [31] I. Mishustin and L. Satarov, Sov. J. Nucl. Phys. **37**, 532 (1983).
- [32] C. M. Hung and E. Shuryak, Phys. Rev. Lett. **75**, 4003 (1995).
- [33] D. H. Rischke and M. Gyulassy, Nucl. Phys. **A597**, 701 (1996); D. H. Rischke, *ibid.* **A610**, 88 (1996).
- [34] P. Koch, B. Muller, and J. Rafelski, Phys. Rep. **142**, 167 (1986).
- [35] J. Letessier, J. Rafelski, and A. Tounsi, Phys. Lett. B **323**, 393 (1994).
- [36] S. Gavin, Nucl. Phys. **A544**, 459 (1992).
- [37] M. Kataja and P. V. Ruuskanen, Phys. Lett. B **243**, 181 (1990).
- [38] E. Shuryak, Phys. Lett. B **207**, 345 (1988); Phys. Rev. D **42**, 1764 (1990).
- [39] P. Gerber, H. Leutwyler, and J. L. Goity, Phys. Lett. B **246**, 513 (1990).
- [40] D. H. Rischke, M. I. Gorenstein, H. Stöcker, and W. Greiner, Z. Phys. C **51**, 485 (1991).
- [41] H. Bebie, P. Gerber, J. L. Goity, and H. Leutwyler, Nucl. Phys. **B378**, 95 (1992).
- [42] E. V. Shuryak, “Event per event analysis of heavy ion collisions and thermodynamical fluctuations,” SUNY-NTG-97-17, hep-ph/9704456.
- [43] Madappa Prakash, Manju Prakash, R. Venugopalan, and G. Welke, Phys. Rep. **227**, 321 (1993).
- [44] Particle Data Group, Phys. Rev. D **54**, 195 (1996).
- [45] F. Grassi, Y. Hama, and T. Kodama, Phys. Lett. B **355**, 9 (1995).
- [46] C. W. Misner, K. S. Thorne, and J. A. Wheeler, *Gravitation* (Freeman, San Francisco, 1973), Chap. 5.